RESEARCH ARTICLE

Establishment and Simulation of Adaptive Strategy for Cancer Therapy Under Multi-Drug Conditions

Hanyin Li[1], **Wanqin Wu**[1,*] **and Xuewen Tan**[1]

[1] School of Mathematics and Computer Science, Yunnan Minzu University, Kunming 650031, China

Abstract

Previous research has focused on formulating cancer treatment strategies within a single-drug framework, which clearly fails to effectively address the practical needs of combination drug therapy in clinical settings. Therefore, this study develops a multi-drug cancer treatment model and conducts strategy design and simulation investigations under hypothetical patient-specific parameters for dual-drug regimens. Based on the previously proposed adaptive threshold strategy and several novel strategies integrating threshold-based and sequential administration patterns, and conducted a parameter search and optimization of upper/lower thresholds was performed to explore the performance improvement of strategies resulting from threshold adjustments in the multi-drug framework. Furthermore, a threshold decay coefficient was introduced to facilitate further optimization and enhance strategy performance. Experimental results demonstrate that the newly proposed multi-drug cancer treatment strategies outperform the extended traditional strategy. Parameter optimization of both thresholds and the threshold decay coefficient improved the survival benefit of the strategies to varying degrees. This indicates that, compared with the traditional parallel multi-drug treatment model, strategies incorporating sequential drug administration characteristics significantly exploit the synergistic effects among drugs, yielding superior therapeutic outcomes.

Keywords: computer simulation, multi-drug cancer therapy, adaptive strategy.

1 Introduction

A major challenge in cancer treatment is the existence of drug resistance [1], which is the primary cause of treatment failure. Existing studies have shown that both intrinsic and acquired drug resistance may influence cancer treatment outcomes [2]. Previous research and development efforts based on therapeutic strategies to overcome drug resistance have yielded generally unsatisfactory results [3, 4]. A strategy based on continuous treatment with maximum tolerated dose (MTD) [5, 6] has significantly improved the possibility of cancer cure, but it is accompanied by an extremely high risk of drug resistance progression. On the other hand, strategies based on the principle of adaptability [7, 8] have delayed the emergence of drug resistance and improved patients' survival [9–

Submitted: 05 December 2025
Accepted: 06 January 2026
Published: 07 March 2026

Vol. 2, **No.** 1, 2026.
10.62762/JNSPM.2025.161987

***Corresponding author:**
✉ Wanqin Wu
041379@ymu.edu.cn

Citation
Li, H., Wu, W., & Tan, X. (2026). Establishment and Simulation of Adaptive Strategy for Cancer Therapy Under Multi-Drug Conditions. *Journal of Numerical Simulations in Physics and Mathematics*, 2(1), 1–8.

12]. Among these, the adaptive threshold strategy (AT50) [13–16] has been extensively studied. Research on the impact of thresholds on treatment outcomes indicates that increasing the threshold can lead to longer survival but also higher progression risk. These studies have so far focused primarily on single-drug frameworks.

In this work, we will introduce multi-drug treatment and combine the classic multi-drug sequential strategy [17] to construct an adaptive strategy under a multi-drug framework. Furthermore, we will explore how changes in the upper and lower thresholds of the adaptive threshold strategy affect treatment outcomes. Incorporating the evolutionary characteristics of drug-resistant cancer cells, we introduce a threshold attenuation coefficient to investigate whether dynamic threshold control can further enhance strategy efficacy. Essentially, we aim to develop a strategy under multi-drug treatment conditions that is similar to adaptive strategies in single-drug frameworks, thereby improving patient survival.

2 Cancer Dynamical Models Under Polypharmacy

We modify the single-drug cancer treatment model in the paper [18] and construct a cancer dynamics model that can characterize the action of n types of drugs, as shown in Equation (1). The meanings of each parameter are listed in Table 1. P is a phenotypic term consisting of an n-dimensional vector of 0s and 1s: the k-th position takes 0 if the cancer cell phenotype is resistant to the k-th type of drug (D_k) and 1 if it is sensitive to D_k. Parameters r, d, and K are consistent with the previous model, representing the birth rate, death rate, and population carrying capacity of different cancer cell phenotypes, respectively. C_k denotes the killing rate of the k-th type of drug (D_k), and a summation is performed for the killing of sensitive phenotypes based on the judgment of phenotype P.

$$\frac{dx_p}{dt} = r_p x_p \left(1 - \frac{\sum_{q\in p} x_q}{K}\right)\left(1 - \sum_{k=1}^{n} s_k C_k\right) - d_p x_p \tag{1}$$

For the convenience of subsequent analysis, we set $n = 2$ (i.e., the cancer treatment model under two drugs) for further investigation.For the dual-drug therapy scenario, the n-dimensional phenotypic vector P in the general form is specified as $P = (s_1, s_2)$, where $s_1, s_2 \in \{0, 1\}$ correspond to the sensitivity states of cancer cells to the two drugs, respectively. Accordingly, the original general symbol x_P is replaced with $x_{(s_1,s_2)}$ to intuitively reflect the correspondence between phenotype and drug sensitivity. Substituting the number of drugs into Equation (1), we obtain four equations (2)–(5) to characterize the cancer treatment model under dual-drug conditions. These four equations correspond to four cancer cell phenotypes: double-sensitive $x_{(1,1)}$, two types of single-sensitive $x_{(1,0)}$ and $x_{(0,1)}$, and double-resistant $x_{(0,0)}$. The killing effect of different drugs only acts on cancer cell populations with sensitive targets, such that the double-resistant phenotype $x_{(0,0)}$ in Equation (5) has no drug inhibition. Additionally, with the increase in the number of drugs, it is no longer feasible to fit parameters using clinical data. Due to the lack of clinical data for multi-drug scenarios, and consistent with previous modeling studies, we adopted hypothetical parameter values based on biological principles. We believe that when transitioning from a single-drug model to a multi-drug model, the main change lies in the addition of new phenotypes, and the core cancer cell phenotypes can be approximated. Therefore, the main parameters (e.g., those for the double-sensitive and double-resistant phenotypes) are partially derived from the values in [18]. Subsequently, the parameters of the newly added phenotypes are assumed based on the principle

Table 1. Symbols and definitions.

Symbol	Meaning	Explanation
$D = \{D_1, \ldots, D_n\}$	Class N Drugs	Set of n drugs.
$P = (s_1, \ldots, s_n)$	Cancer Cell Phenotype	Phenotype vector, where $s_k \in \{0, 1\}$.
$s_k = 1$	Sensitivity to D_k	Indicates the cancer cell is sensitive to drug D_k.
$s_k = 0$	Resistance to D_k	Indicates the cancer cell is resistant to drug D_k.
$\rho = \{0, 1\}^n = 2^n$	Total Number of Phenotypes	All combinations of sensitive/resistant phenotypes for n drugs.
$C_k \geq 0$	Killing Coefficient of D_k	Toxicity coefficient of the k-th drug.
$x_p(t)$	Population of P-phenotype Cancer Cells	Time-dependent population of phenotype P cancer cells.
r_p	Growth Rate of P-phenotype Cancer Cells	Intrinsic growth rate of phenotype P cancer cells.
d_p	Death Rate of P-phenotype Cancer Cells	Natural death rate of phenotype P cancer cells.
K	Carrying Capacity	Environmental limit for total cancer cell population.

Table 2. Core parameter values of the cancer drug strategy model.

Parameter Name	Value	Physical Meaning
$r_{(1,1)}$	0.027	Basal growth rate of dual-sensitive cells $(x_{(1,1)})$
$r_{(1,0)}$	0.021	Basal growth rate of F-only sensitive cells $(x_{(1,0)})$
$r_{(0,1)}$	0.020	Basal growth rate of D-only sensitive cells $(x_{(0,1)})$
$r_{(0,0)}$	0.015	Basal growth rate of dual-resistant cells $(x_{(0,0)})$
$x_{(1,1)0}$	0.8595	Initial quantity of dual-sensitive cells $(x_{(1,1)})$
$x_{(1,0)0}$	0.0021	Initial quantity of F-only sensitive cells $(x_{(1,0)})$
$x_{(0,1)0}$	0.0024	Initial quantity of D-only sensitive cells $(x_{(0,1)})$
$x_{(0,0)0}$	0.0015	Initial quantity of dual-resistant cells $(x_{(0,0)})$
C_1	1.5	Growth inhibition coefficient of Drug D
C_2	1.2	Growth inhibition coefficient of Drug F
$d_{(1,1)}$	0.001	Basal death rate of dual-sensitive cells $(x_{(1,1)})$
$d_{(1,0)}$	0.001	Basal death rate of F-only sensitive cells $(x_{(1,0)})$
$d_{(0,1)}$	0.001	Basal death rate of D-only sensitive cells $(x_{(0,1)})$
$d_{(0,0)}$	0.001	Basal death rate of dual-resistant cells $(x_{(0,0)})$
K	1.5	Carrying capacity

of cost: this principle requires that as the number of drug-resistant targets increases, the proliferation rate of cancer cells decreases accordingly.Detailed parameter values are given in Table 2.

$$\frac{dx_{(1,1)}}{dt} = r_{(1,1)}x_{(1,1)}\left(1 - \frac{x_{(0,0)} + x_{(0,1)} + x_{(1,0)} + x_{(1,1)}}{K}\right) \times (1 - C_1 - C_2) - d_{(1,1)}x_{(1,1)}, \quad (2)$$

$$\frac{dx_{(1,0)}}{dt} = r_{(1,0)}x_{(1,0)}\left(1 - \frac{x_{(0,0)} + x_{(0,1)} + x_{(1,0)} + x_{(1,1)}}{K}\right) \times (1 - C_1) - d_{(1,0)}x_{(1,0)}, \quad (3)$$

$$\frac{dx_{(0,1)}}{dt} = r_{(0,1)}x_{(0,1)}\left(1 - \frac{x_{(0,0)} + x_{(0,1)} + x_{(1,0)} + x_{(1,1)}}{K}\right) \times (1 - C_2) - d_{(0,1)}x_{(0,1)}, \quad (4)$$

$$\frac{dx_{(0,0)}}{dt} = r_{(0,0)}x_{(0,0)}\left(1 - \frac{x_{(0,0)} + x_{(0,1)} + x_{(1,0)} + x_{(1,1)}}{K}\right) - d_{(0,0)}x_{(0,0)}. \quad (5)$$

3 Threshold Screening for Upper and Lower Bounds

First, we elaborate on the strategy benefit to facilitate a quantitative comparison of the effectiveness of subsequent strategy optimization efforts; the strategy benefit is primarily characterized by the extension in survival time achieved by the improved strategy compared to the original one, where survival time in simulations is defined as the duration required for the total cancer volume N to reach the termination threshold of 1.2, a parameter set in accordance with the construction principles outlined in [18]. Subsequent work will focus on two key aspects: the survival time of the novel strategy formulated by incorporating the sequential mode outperforms that of the traditional parallel adaptive strategy mode, and the survival time of the strategy after parameter optimization exceeds that of the strategy under the original parameter conditions. In summary, the strategy benefit reflects the difference in the time required to reach the simulation termination point across different strategies, which objectively demonstrates the positive impacts brought about by strategy optimization.

In terms of screening the upper and lower thresholds for strategy control,we extend the AT50 threshold strategy under the single-drug framework to the dual-drug framework and construct the strategy method as shown in Figure 1(A). Second, We integrate the sequential mode from the periodic strategy proposed in the existing multi-drug framework [17] with the threshold control method.Namely those depicted in Figure 1(D, G, J).The legend explanations for the simulation images of these strategies are presented in Figure 1(M).The strategies depicted in panels (D, G, J) of Figure 1 are all formulated by integrating the threshold-controlled characteristics of the AT50 strategy and the sequential approach of the periodic strategy.Specifically, through the differential combination of threshold control methods and drug sequential orders, we switch the type of drug used at the drug failure node, which distinguishes it from the traditional concurrent processing mode. It should be noted that the drug failure node here is described as a state where cancer cells with sensitive phenotypes to a certain type of drug are on the verge of extinction

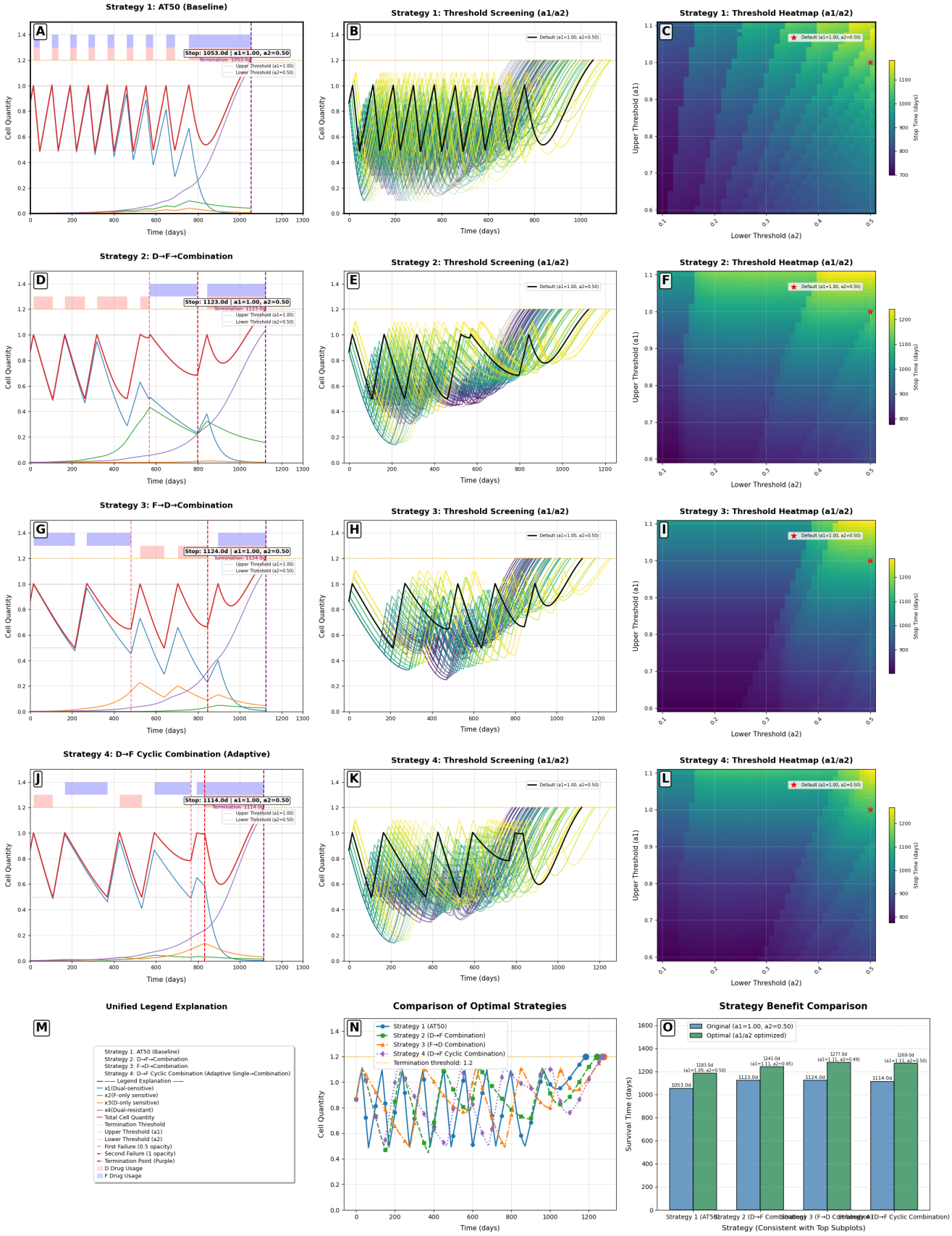

Figure 1. Numerical simulation results of screening and optimization for upper and lower threshold control parameters under several strategies.

under the continuous killing effect of that drug. At this point, it is reflected in the model as a node where the drug loses its inhibitory effect. The two strategies depicted in Figure 1(D, G) differ in the order of drug administration, but they are essentially constructed under the single sequential administration mode. Two drug failure nodes are marked in the simulation: after the first failure node, another type of drug is adopted when the system recovers to the threshold. After the second failure node, since both drugs have lost their original killing advantages to varying degrees, the traditional concurrent mode is used in the final stage for ultimate inhibitory killing. The strategy described in Figure 1(J) is similar to this, with the difference that a continuous sequential administration mode is adopted. Simulations show that the continuous sequential administration mode is slightly less effective than the other two administration modes; even so, it still achieves a strategy benefit of more than 50 days higher than that of the traditional AT50 strategy.

In the threshold strategy, the core parameters influencing a patient's survival time are the upper threshold a_1 and the lower threshold a_2. Therefore, we performed a parameter search on the thresholds of the four strategies (A, D, G, J) to obtain the optimal control parameters, thereby delaying the progression of drug resistance as much as possible and achieving the goal of prolonging the patient's survival time. In this study, the search range for the upper threshold is set as $a_1 = [0.5, 1]$, the search range for the lower threshold is $a_2 = [0.1, 0.5]$, and the search step size is 0.01. Figure 1(B, E, H, K) illustrate the strategy simulation trajectories under varying parameters, where the black trajectory represents the simulation result under the control of the original threshold $[a_1, a_2] = [1, 0.5]$.The yellow trajectories represent the control methods whose strategy benefits exceed the default threshold parameters, while the green trajectories correspond to those underperforming the model parameters. Simulations of cancer cell treatment trajectories for the four strategies under different threshold parameters all indicate that the threshold parameters indeed contain key components for further improving the effectiveness of the strategies.

Figure 1(C, F, I, L) are heatmaps of the survival benefits of different strategies when the upper and lower thresholds change, with the red asterisk indicating the benefit corresponding to the original threshold. The imaging results demonstrate that the search for the upper and lower thresholds effectively prolongs the patient's survival time. The simulation results of the optimal parameter combinations obtained through the search for the four strategies are shown in Figure 1(N); it can be observed that the three schemes combining the periodic strategy and the threshold strategy are all superior to the extended AT50 strategy.

The comparison results of the benefits of different strategies and the effectiveness of the threshold screening work are presented in Figure 1(O), the benefit comparison of the original blue strategies without threshold parameter optimization shows that the three control strategies combining sequential administration and thresholding all outperform the concurrent AT50 strategy by more than 50 days.This indicates that compared with concurrent administration, the sequential administration modes of the two drugs exert a stronger competitive inhibitory effect on drug-resistant cancer cells. This is because the multi-drug sequential mode enables each subpopulation of sensitive cancer cells to gain greater competitive advantages. The similar strategy benefits of Original Strategy 2 and Strategy 3 in Figure 1(O) illustrate that under the sequential mode, changing the order of drug administration does not have a significant impact on the strategy benefits. Finally, the green section presents the performance improvement results of the strategies after threshold parameter optimization. It can be clearly observed that the three newly constructed strategies still outperform the traditional AT50 strategy in terms of benefits. Furthermore, the optimization of threshold parameters leads to a performance improvement of more than 150 days for the AT50 strategy, while the other strategies generally achieve a performance enhancement of over 100 days. This indicates that under the multi-drug cancer model, the optimization of threshold parameters can indeed greatly tap into the potential performance benefits of the strategies.

4 Threshold Attenuation Coefficient: Introduction and Screening

The method of using fixed upper and lower thresholds loses a certain degree of adaptability to the changes in cancer cells. Specifically, as cancer progresses, the proportion of drug-resistant cancer cells increases, and the continued use of fixed thresholds will make it difficult to cope with this situation. Here, we introduce threshold attenuation coefficients into the upper and lower threshold control parameters to dynamically adapt to changes in drug-resistant cancer cells, aiming to achieve the maximum competitive inhibition effect. In this section, we conduct a screening

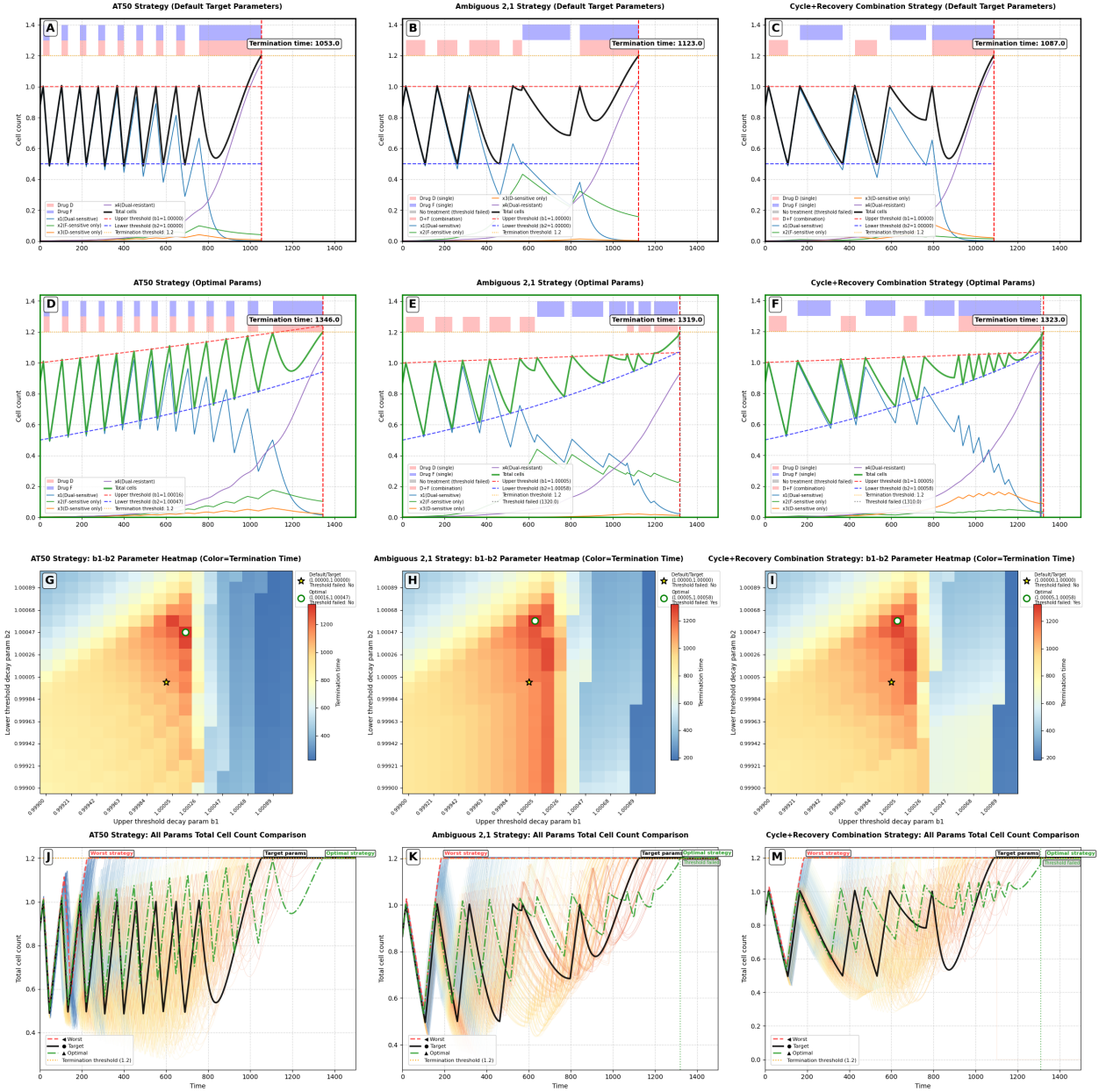

Figure 2. Numerical simulation results under parameter optimization with the introduction of a threshold decay coefficient.

of threshold attenuation coefficients for the previously mentioned AT50 strategy and two newly developed control strategies. The initial value ranges for both the upper threshold attenuation coefficient and the lower threshold attenuation coefficient are set to $[0.9990, 1.0010]$, with a search step size of 0.0001.

The first row of subfigures in Figure 2 simulate the results of the three original strategies under the default threshold attenuation coefficient conditions. At this point, the default target parameters of the threshold attenuation coefficients $[b_1, b_2]$ for the three simulated strategies are set to $[1, 1]$. Figure 2(A) shows the threshold control method extended to the dual-drug framework, while Figure 2(B, C) represent two new strategies we developed by combining the characteristics of threshold strategies and sequential strategies. Figure 2(D, E, F) present simulations of the optimal strategies under the searched best threshold attenuation coefficients. The results indicate that the introduction of attenuation coefficients significantly improves the performance of the original strategies. Figure 2(G, H, I) provide examples of heatmaps during the threshold attenuation coefficient screening process, where the abscissa denotes the lower threshold attenuation coefficient, the ordinate represents the upper threshold attenuation coefficient, and the color difference reflects the survival benefit of the

strategy under different parameter combinations. The heatmaps for all three strategies demonstrate that there exists a set of threshold attenuation coefficient combinations that can further enhance the strategy performance. Figure 2(J, K, M) illustrate the change trajectories of the overall cancer cell volume under the three strategies during the variation of attenuation coefficients. Default Parameter Strategy are plotted in black, while the optimal control strategies are shown in green.

5 Conclusion

Research results indicate that both the AT50 strategy extended to the dual-drug framework and several strategies we developed by integrating traditional threshold control methods with sequential strategies have achieved varying degrees of improvement in strategy benefits during the optimization of the strategies' upper and lower threshold control parameters. Furthermore, the additional optimization with the introduction of a threshold decay coefficient has yielded even more significant improvements in strategy benefits across all original strategies. On the other hand, the newly developed multi-drug control strategies, like the traditional AT50 strategy, can regulate drug administration based on clinically monitored cancer cell volume. Such mathematical model-independent interactive control strategies offer valuable guidance for multi-drug therapy.

However, under the assumed cancer patient parameter conditions, the newly developed control strategies only approached the survival benefit of the extended AT50 strategy. Through analysis, we found that in multi-drug therapy scenarios, the additional benefits of the new strategies integrated with sequential methods mainly stem from the interaction of the two drugs to maintain the competitive dominance of the three types of sensitive cancer cells. Therefore, this result arises because the proportional composition of the two types of single-sensitive cells in the assumed patient parameters is nearly consistent with that of dual-resistant cells. In future research, we need to formulate strategies under a broader range of cancer patient parameter conditions to enhance the generalization ability of the strategies. Moreover, in more drug therapy scenarios, exploring the population competitive advantage of sensitive cancer cell phenotypes to a greater extent can greatly improve drug efficacy, achieving a treatment mode superior to traditional parallel multi-drug therapy.

Data Availability Statement

Data will be made available on request.

Funding

This work was supported in part by the National Natural Science Foundation of China under Grant 11361104 and Grant 12261104; in part by the Youth Talent Program of Xingdian Talent Support Plan under Grant XDYC-QNRC 2022-0514; in part by the Yunnan Provincial Basic Research Program Project under Grant 202301AT070016 and Grant 202401AT070036; in part by the Yunnan Province International Joint Laboratory for Intelligent Integration and Application of Ethnic Multilingualism under Grant 202403AP140014.

Conflicts of Interest

The authors declare no conflicts of interest.

AI Use Statement

The authors declare that Doubao 1.8 was used for cross-lingual translation and grammatical correction during the preparation of this manuscript. The authors reviewed and edited the output as necessary and take full responsibility for the final content of the manuscript.

Ethical Approval and Consent to Participate

Not applicable. This is a purely computational and mathematical modeling study with no involvement of human or animal subjects; therefore, ethical approval is not required.

References

[1] Bukowski, K., Kciuk, M., & Kontek, R. (2020). Mechanisms of multidrug resistance in cancer chemotherapy. *International Journal of Molecular Sciences, 21*(9), 3233. [CrossRef]

[2] Holohan, C., Van Schaeybroeck, S., Longley, D. B., & Johnston, P. G. (2013). Cancer drug resistance: An evolving paradigm. *Nature Reviews Cancer, 13*(10), 714-726. [CrossRef]

[3] Ganesh, K., & Massagué, J. (2021). Targeting metastatic cancer. *Nature Medicine, 27*(1), 34-44. [CrossRef]

[4] Tevaarwerk, A. J., Gray, R. J., Schneider, B. P., Smith, M. L., Wagner, L. I., Fetting, J. H., & ... (2013). Survival in patients with metastatic recurrent breast cancer after adjuvant chemotherapy: Little evidence of improvement over the past 30 years. *Cancer, 119*(6), 1140-1148. [CrossRef]

[5] Gatenby, R. A., & Brown, J. S. (2020). The evolution and ecology of resistance in cancer therapy. *Cold Spring Harbor Perspectives in Medicine, 10*(11), a040972. [CrossRef]

[6] Gillies, R. J., Verduzco, D., & Gatenby, R. A. (2012). Evolutionary dynamics of carcinogenesis and why targeted therapy does not work. *Nature Reviews Cancer, 12*(7), 487-493. [CrossRef]

[7] Zhang, J., Cunningham, J. J., Brown, J. S., & Gatenby, R. A. (2017). Integrating evolutionary dynamics into treatment of metastatic castrate-resistant prostate cancer. *Nature Communications, 8*(1), 1816. [CrossRef]

[8] Zhang, J., Cunningham, J., Brown, J., & Gatenby, R. (2022). Evolution-based mathematical models significantly prolong response to abiraterone in metastatic castrate-resistant prostate cancer and identify strategies to further improve outcomes. *Elife, 11*, e76284. [CrossRef]

[9] Martin, R. B., Fisher, M. E., Minchin, R. F., & Teo, K. L. (1992). Optimal control of tumor size used to maximize survival time when cells are resistant to chemotherapy. *Mathematical biosciences, 110*(2), 201-219. [CrossRef]

[10] Monro, H. C., & Gaffney, E. A. (2009). Modelling chemotherapy resistance in palliation and failed cure. *Journal of theoretical biology, 257*(2), 292-302. [CrossRef]

[11] Gatenby, R. A., Silva, A. S., Gillies, R. J., & Frieden, B. R. (2009). Adaptive therapy. *Cancer research, 69*(11), 4894-4903. [CrossRef]

[12] Hansen, E., Woods, R. J., & Read, A. F. (2017). How to use a chemotherapeutic agent when resistance to it threatens the patient. *PLOS Biology, 15*(2), e2001110. [CrossRef]

[13] Strobl, M. A., West, J., Viossat, Y., Damaghi, M., Robertson-Tessi, M., Brown, J. S., ... & Anderson, A. R. (2021). Turnover modulates the need for a cost of resistance in adaptive therapy. *Cancer research, 81*(4), 1135-1147. [CrossRef]

[14] Hansen, E., & Read, A. F. (2020). Modifying adaptive therapy to enhance competitive suppression. *Cancers, 12*(12), 3556. [CrossRef]

[15] Viossat, Y., & Noble, R. (2021). A theoretical analysis of tumour containment. *Nature ecology & evolution, 5*(6), 826-835. [CrossRef]

[16] Kim, E., Brown, J. S., Eroglu, Z., & Anderson, A. R. (2021). Adaptive therapy for metastatic melanoma: predictions from patient calibrated mathematical models. *Cancers, 13*(4), 823. [CrossRef]

[17] West, J., You, L., Zhang, J., Gatenby, R. A., Brown, J. S., Newton, P. K., & Anderson, A. R. (2020). Towards multidrug adaptive therapy. *Cancer research, 80*(7), 1578-1589. [CrossRef]

[18] Gallagher, K., Strobl, M. A., Park, D. S., Spoendlin, F. C., Gatenby, R. A., Maini, P. K., & Anderson, A. R. (2024). Mathematical model-driven deep learning enables personalized adaptive therapy. *Cancer Research, 84*(11), 1929-1941. [CrossRef]

Hanyin Li is a graduate student at the School of Mathematics and Computer Science,Yunnan Minzu University.Affiliation:School of Mathematics and Computer Science,Yunnan Minzu University,Kunming,Yunnan Province,P.R. China.(Email: 2294067171@qq.com)

Wanqin Wu received a Master of Science (M.Sc.) degree from the School of Mathematics and Statistics,Yunnan University in July 2009.Affiliation:School of Mathematics and Computer Science,Yunnan Minzu University, Kunming,Yunnan Province,P.R. China.(Email: 041379@ymu.edu.cn)

Xuewen Tan received a Doctor of Science (Sc.D.) degree in Computational Mathematics from Shaanxi Normal University in 2018.Affiliation:School of Mathematics and Computer Science,Yunnan Minzu University,Kunming,Yunnan Province,P.R. China.(Email: tanxw0910@ymu.edu.cn)